Life Sciences 234 (2019) 116778

Contents lists available at ScienceDirect

Life Sciences

journal homepage: www.elsevier.com/locate/lifescie

Proteomic analysis of the intestine reveals SNARE-mediated immunoregulatory and amino acid absorption perturbations in a rat model of depression

Xue Gong[a,b,c,1], Cheng Huang[a,b,c,1], Xun Yang[a,b,c,1], Qiang Mao[d,1], Li Zeng[a,e], Peng Zheng[a,b,c], Juncai Pu[a,b,c], Jianjun Chen[a,b], Haiyang Wang[a,b], Bing Xu[a,b,c], Chanjuan Zhou[a,b], Peng Xie[b,c,f,g,h,i,*]

[a] Institute of Neuroscience and the Collaborative Innovation Center for Brain Science, Chongqing Medical University, Chongqing, China
[b] Chongqing Key Laboratory of Neurobiology, Chongqing 400016, China
[c] Department of Neurology, the First Affiliated Hospital of Chongqing Medical University, Chongqing, China
[d] Department of Pharmacy, the Second Affiliated Hospital of Chongqing Medical University, Chongqing 400010, China
[e] Department of Nephrology, the Second Affiliated Hospital of Chongqing Medical University, Chongqing 400010, China
[f] Department of Neurology, Yongchuan Hospital, Chongqing Medical University, Chongqing 402160, China
[g] Key Laboratory of Clinical Laboratory Diagnostics, Ministry of Education, Chongqing, China
[h] South Australian Health and Medical Research Institute, Mind and Brain Theme, Adelaide, SA, Australia
[i] Flinders University, Adelaide, SA, Australia

ARTICLE INFO

Keywords:
Depression
Intestine
SNARE
Immunoregulation
Amino acid
Gut-brain axis

ABSTRACT

Aims: To clarify the role of the gut-brain axis in depression.
Main methods: We used the iTRAQ technique to identify differential proteins in the intestine of the rat model of chronic unpredictable mild stress (CUMS)-induced depression. Significant differential proteins were subjected to Gene Ontology (GO) functional annotations and KEGG pathway enrichment analysis. Key proteins were validated at the mRNA and protein levels. The levels of cytokines in the intestine, serum and hypothalamus were examined by ELISA. HPLC-UV was used to detect the levels of amino acids.
Key findings: In the rat intestine, 349 differential proteins (209 downregulated, 140 upregulated) were identified. GO analysis indicated that "protein complex assembly" was the first-ranked biological process. SNARE complex components, including SNAP23, VAMP3 and VAMP8, were increased at the mRNA levels, while only VAMP3 and VAMP8 were also upregulated at the protein level. TNFα, IL6 and IL1β were upregulated in the CUMS rat intestine, while TNFα was decreased in the serum and hypothalamus. IL1β was decreased in the serum. "Protein digestion and absorption" was the most significantly enriched KEGG pathway, involving 5 differential proteins: SLC9A3, ANPEP, LAT1, ASCT2 and B^0AT1. Glutamine, glycine and aspartic acid were perturbed in the CUMS rat intestine.
Significance: Our findings suggest that CUMS enhances the adaptive immune response in the intestine through ER-phagosome pathway mediated by SNARE complex and disturb absorption of amino acids. It advances our understanding of the role of gut-brain axis in depression and provides a potential therapeutic target for the disease.

1. Introduction

Major depressive disorder (MDD) is an increasingly prevalent mental disorder that severely impacts the quality of life of patients and impacts a huge economic burden on individuals and society [1–3]. Numerous studies have investigated the mechanisms of depression [4–7]; however, the pathogenesis of the disorder remains unclear.

Accumulating evidence suggests that "the gut-brain axis, a concept that" highlights the bidirectional communication between the intestinal microbiota and CNS, plays a critical role in neuropsychiatric disorders

* Corresponding author at: Department of Neurology, the First Affiliated Hospital, Chongqing Medical University, No. 1 Yixueyuan Road, Yuzhong District, Chongqing 400016, China.
E-mail address: xiepeng@cqmu.edu.cn (P. Xie).
[1] These authors contributed equally to this work.

https://doi.org/10.1016/j.lfs.2019.116778
Received 15 May 2019; Received in revised form 8 August 2019; Accepted 16 August 2019
Available online 17 August 2019

[8–11]. Clinical studies have demonstrated disturbances in the gut microbiotic composition in depressive patients, similar to those observed in rodent models of depression [12–15]. In our previous study, we pioneered the fecal transplantation model of depression by transferring the feces of MDD patients to germ-free mice to introduce depressive-like behaviors in the animals [16]. These preliminary findings suggest that there is a causal connection between alterations in the gut microbiota and depression.

The intestine is colonized by a large diversity of microorganisms [17]. The intestinal mucosal layer, as the first line of host defense, normally forms an effective barrier to limit interactions between microbiota, microbial toxins, pathogenic antigens and the lamina propria [18,19]. This barrier is composed of simple columnar cells held together by tight junctions, restricting the movement of substances across the epithelial cell layers [19]. However, stress can induce activation of the hypothalamic-pituitary-adrenal (HPA) axis and sympathetic nervous system (SNS) signaling, thereby weakening tight junctions and perturbing intestinal permeability [20]. The ensuing translocation of luminal microbial antigens can trigger a local immune response, which may in turn activate Myosin Light Chain Kinase (MLCK), resulting in systemic inflammation [20]. Indeed, a clinical study of adolescent depression suggests that intestinal permeability might be associated with the severity of neurovegetative symptoms, likely via the innate immune system [21]. Thus, the gut-brain axis may play a key pathogenetic role in depression.

The chronic unpredictable mild stress (CUMS) paradigm is the most widely used rodent model of depression [22,23], and it emphasizes the role of stress in the etiology of depression. Isobaric tags for relative and absolute quantification (iTRAQ) is an advanced technique used for relatively protein quantitative analysis, with features of high accuracy, sensitivity and reproducibility [23,24]. Therefore, in this study, we used iTRAQ to identify the changes in protein profiles in the intestine of the CUMS rat model of depression., We followed this with RT-qPCR, western blotting, ELISA and HPLC for validation, in an effort to provide insight into the intestinal functional alterations and changes in the gut-microbiota system in depression. Our study represents a new approach for understanding the pathogenesis of depression and provides insight into the role of the gut-brain axis in the disease.

2. Materials and methods

2.1. Experimental design

The present study was conducted to detect intestinal proteins that might contribute to depression-like behaviors to clarify the pathogenesis of depression. Differential proteins in the CUMS intestine were identified by iTRAQ and analyzed by DAVID and KEGG, to elucidate protein functions and signaling pathways. Based on the bioinformatics analysis, we focused on the top 1 biological process of “protein complex assembly” and selected proteins in this biological process for further analysis and validation. At the transcript and protein levels, SNAP23, VAMP3 and VAMP8, components of the SNARE complex, were validated as substantially altered. Because the SNARE complex participates in the antigen presenting process in the immune response, we performed ELISA to detect changes in the levels of cytokines in the intestine, serum and hypothalamus, which may reflect interactions within the gut-blood-brain axis. Based on KEGG pathway analysis, “protein absorption” was top-ranking. Therefore, using the HPLC-UV method, we examined the levels of amino acids. The experimental design is presented as a flowchart (Fig. 1).

2.2. Animals and ethics statement

Male Sprague-Dawley rats, weighing 180–240 g and 8–10 weeks of age, were purchased from the Laboratory Animal Center of Chongqing Medical University. All animals were individually housed under

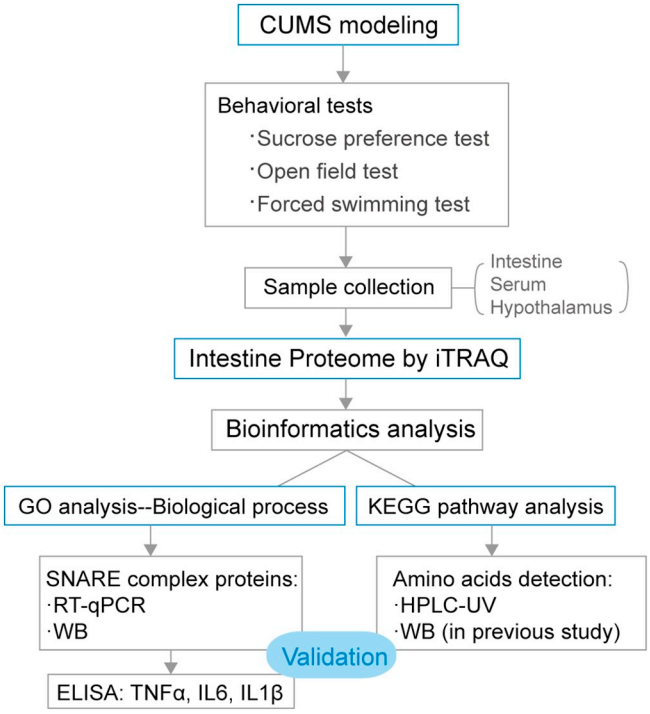

Fig. 1. Flow chart of the experimental design.

standard conditions with a 12-h light/dark cycle (lights on at 7:30 am), temperature of 22 ± 1 °C, humidity of 52 ± 2%, and with free access to food and water (except for experimental animals subjected to food and water deprivation stressors in the CUMS procedure). This study was approved by the Ethics Committee of Chongqing Medical University, and all animal handling and treatment procedures were in accordance with the National Institutes of Health Guidelines for Animal Research (*Guide for the Care and Use of Laboratory Animals*, NIH Publication No. 8023, revised 1996). Special care was taken to minimize the number and suffering of animals.

2.3. CUMS procedure

The CUMS procedure was conducted according to our previous study [25] with minor modification. After 1 week of adaptation, all animals were randomly assigned to the CUMS experimental group (CUMS, $n = 20$) or the non-stress control group (CON, $n = 20$), and were matched for body weight and sucrose preference. Rats in the CUMS group were subjected to 4 weeks of chronic unpredictable mild stress, as shown in Fig. 2A. Each rat in the CUMS group received 1 or 2 stressors per day, but the same stressor was not applied for 2 consecutive days (Supplementary Table S1). At the end of the CUMS period, the rats were deprived of food and water for 24 h (deemed the final stressor in the CUMS group) prior to behavioral testing. Rats in the control group were not disturbed during the 4-week period, with ad libitum access to food and water, and they were isolated from the stressed animals, to avoid any acoustic or olfactory communication between the groups.

2.4. Behavioral tests

2.4.1. Sucrose preference test (SPT) and body weight

The SPT was used to assess anhedonia, an index of depressive-like behavior [25]. Seventy-two hours before the first round of SPT, all rats were trained as follows: two bottles of 1% sucrose solution were placed in the cage, and then, 24 h later, one was replaced with a bottle of tap water. In the last 24-h period, rats were deprived of food and water.

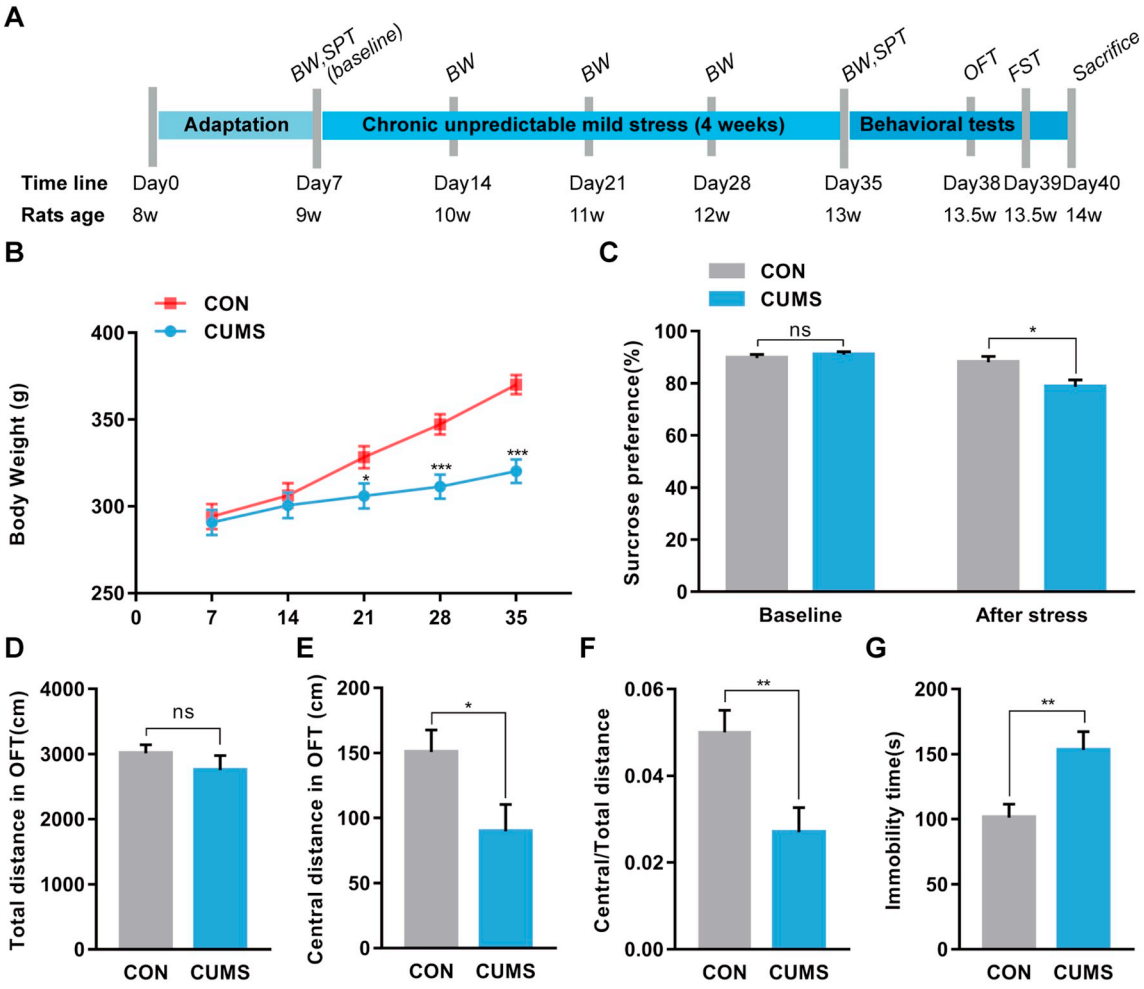

Fig. 2. CUMS induces depressive- and anxiety-like behaviors in rats. (A) Diagram of the CUMS procedure. After one week of adaptation, body weight was measured and the sucrose preference test was performed, as baseline indices. Subsequently, rats in the CUMS group were subjected to four weeks of CUMS exposure. All rats were sacrificed after 3 days of behavioral tests (BW, SPT, OFT, FST). (B) BW: No significant difference at baseline (day 7), but a marked reduction from the second week (day 21) until the end of the CUMS procedure was observed. (C) SPT: No difference at baseline, but a reduction after stress was observed. (D-F) OFT: No difference was observed in total distance travelled in the OFT (D), but a significant decrease was observed in central distance (E). Furthermore, a remarkable decrease was also observed in the ratio of the central distance to total distance (F). (G) FST: Rats in the CUMS group showed significantly increased immobility time. All data are presented as mean ± SEM ($n = 20$ in the control group; $n = 20$ in the CUMS group). Student's *t*-test; $^{*}p < 0.05$, $^{**}p < 0.01$, ns = no significance. CON, rats in the control group; CUMS, rats in the CUMS group.

After adaptation, a bottle containing 1% sucrose solution and another containing pure water were randomly placed on the left or right side of the cage to eliminate side preference. The 24-h consumptions of 1% sucrose solution and pure water were assessed. Sucrose preference was defined as [sucrose intake / (sucrose intake + water intake)]. The SPT was performed immediately before and after the CUMS procedure. Body weight was measured weekly.

2.4.2. Open field test (OFT)

The OFT was conducted as previously described [26]. Briefly, rats were individually placed in the center of a black box (100 cm × 100 cm × 40 cm box) with the head towards the same direction. After a 30-s latency, locomotor activity and movements in the central zone over a 5-min period were measured. The box was cleaned with alcohol between tests to remove olfactory cues.

2.4.3. Forced swimming test (FST)

The FST was used to assess depressive-like behavior [16]. In the FST procedure, rats were placed individually in a Plexiglas cylinder (50 cm in height × 20 cm in diameter) filled with water (24 ± 1 °C) to a depth of 30 cm. Total immobility time in a 5-min period was calculated. The water was completely replaced after each test. All behavioral tests (OFT and FST) were analyzed by SMART 2.5 software (Panlab SL, Barcelona, Spain).

2.5. Sample collection

After the behavioral tests were completed, rats were anesthetized. Blood was collected via cardiac puncture under deep anesthesia and then centrifuged to isolate serum. After that, rats were sacrificed by dislocation of the cervical vertebrae. Hypothalamic tissues were then harvested from the brain. A 5-cm segment of the distal intestine (1 cm from the cecum) was removed, and the contents were cleared. All samples were rapidly frozen with liquid nitrogen and stored at −80 °C until assay.

2.6. iTRAQ of CUMS intestinal samples

2.6.1. Protein preparation and iTRAQ sample labeling

The iTRAQ procedure was performed as in our previous study [22,24]. Frozen CUMS intestine samples ($n = 10/10$, random samples) were dissolved in SDT buffer, dissociated by sonication, incubated in

Table 1
Primer pairs for RT-qPCR in rat intestine.

Gene	Forward primer (from 5′ to 3′)	Reverse primer (from 5′ to 3′)
Pf4	ATCCATCTCAAACGCATCACC	TACAGAGGTACTTGCCGGTCCA
Pex14	AAGGCTACCACATCAACCAAC	CTCCGATTCAGAAGAAGTCCT
Snap23	TCTGCGTCTGCCCTTGTAAT	TGTTATCCGGCTTGGTTGCT
Vamp3	CTGCAAGATGTGGGCGATAGG	CCGTCAGGCTTCATTTCCTCT
Vamp8	AAGCCACGTCTGAACACTTC	TGCCCGTAGCAAAGAGTATGA
Slc2a1	ACAGAACGTCCATTCTCCGT	ACTCCTCAATTACCTTCTGGGG
β-actin	CCCGCGAGTACAACCTTCTT	CCATCACACCCTGGTGCCTA

Pf4, platelet factor 4; *Pex14*, peroxisomal membrane protein PEX14; *Snap23*, synaptosomal-associated protein; *Vamp3*, vesicle-associated membrane protein 3; *Vamp8*, vesicle-associated membrane protein 8; *Slc2a1*, solute carrier family 2, facilitated glucose transporter member 1.

boiling water, and centrifuged to obtain supernatants. Proteins were quantified with the BCA assay, and then, supernatants collected from three or four rats were pooled as one biological sample to eliminate individual differences, resulting in three biological replicates in each group. Pooled samples were digested into peptides with trypsin, and then labeled using the iTRAQ Reagent-8plex Multiplex Kit (AB SCIEX, Framingham, USA) according to the manufacturer's protocol.

2.6.2. Strong cation exchange chromatography (SCX) fractionation

Labeled peptides were combined into one sample mixture and then fractionated using AKTA Purifier 100 (GE Healthcare, Buckinghamshire, UK). The sample mixtures were purified using a Polysulfoethyl 4.6 × 100 mm column (5 μm, 200 Å) (PolyLC Inc., Maryland, USA) using linear gradient elution at a flow rate of 1 mL/min. The absorbance at 214 nm was monitored during the elution process, and the eluates were collected every 1 min. A total of 30 fractions were collected and combined into 15 pools, followed by desalination on C18 cartridges (66872-U, Sigma, USA).

2.6.3. Liquid chromatography-tandem mass spectrometry (LC-MS/MS) analysis

The desalted peptides were separated on a Thermo EASY nLC system (Thermo Fisher Scientific, Waltham, MA, USA). Samples were trapped on a nanoViper C18 column (Thermo Scientific Acclaim PepMap100, 100 μm × 2 cm) and separated on an analytical column (Thermo Scientific EASY column, 10 cm, ID 75 μm, 3 μm, C18-A2) using linear gradient elution with a flow rate of 300 nL/min. For peptide detection, a Q Exactive mass spectrometer (Thermo Fisher Scientific) was operated in the positive ion full scan mode, and one MS scan with a range of 300–1800 (m/z) and a resolution of 70,000 at m/z 200 was obtained. The top 10 most abundant precursor ions were selected for MS2 fragmentation by higher-energy collision dissociation (HCD). MS2 scans were acquired with a resolution of 17,500 at m/z 200 and an isolation window of m/z 2. The maximum ion inject time (IT) for the full MS scan and the MS2 scans were 10 ms and 60 ms, respectively. The automatic gain control (AGC) target values for both were set to 3×10^6.

2.6.4. iTRAQ protein identification and quantification

MS/MS spectra were searched using MASCOT 2.2 (Matrix Science, London, UK) embedded into Proteome Discoverer 1.4 (Thermo Fisher Scientific) against the Uniprot rat database (Uniprot_Rat_35947_20160706.fasta, downloaded from http://www.uniprot.org). For protein identification, the Mascot search parameters were set as follows: Enzyme: Trypsin; Peptide mass tolerance: 20 ppm; Fragment mass tolerance: 0.1 Da; Max missed cleavages: 2; Fixed modifications: Carbamidomethyl (C), iTRAQ8plex (K), iTRAQ8plex (N-term); Variable modifications: Oxidation (M), iTRAQ8plex (Y); Peptide false discovery rate (FDR) ≤ 0.01. For protein quantification, the protein ratios were calculated as the median of only unique peptides of the protein. All peptide ratios were normalized to the median protein ratio. The median protein ratio should be 1 after normalization.

2.7. Bioinformatics analysis

Proteins with a greater than ± 1.2-fold change, with a P-value < 0.05, were considered differentially expressed and were studied further [22]. All significant proteins were uploaded to DAVID (https://david.ncifcrf.gov/) for Gene Ontology (GO) functional annotations of biological process, molecular function and cellular component. Pathways enrichment analysis was performed based on the KEGG database.

2.8. RT-qPCR

RNAs were extracted from the intestinal tissues of rats using Trizol reagent (Invitrogen, CA, USA) and estimated by Nanodrop. RNAs were reverse-transcribed with the PrimerScript RT reagent Kit with gDNA Eraser (Takara, Dalian, China), following the protocol provided by the manufacturer. RT-qPCR was conducted using the LightCycler 96 system (Roche, Germany) with SYBR Premix Ex Taq (Takara). The primers were designed using BLAST (https://blast.ncbi.nlm.nih.gov/Blast.cgi) and commercially synthesized by TsingKe Biological Technology (Beijing, China). The primer sequences of rats are given in Table 1. Target RNA levels were normalized to *β-actin*.

2.9. Western blotting

Western blotting is a widely used and classical method for protein validation [25]. Frozen intestinal tissues from the CUMS model were washed twice with cold PBS, lysed with RIPA buffer (Beyotime, Shanghai, China) containing 1% PMSF, ultrasonicated on ice, and centrifuged at 14,000 × g for 5 min at 4 °C to remove insoluble material. Total proteins were quantified using the BCA method before denaturation. Samples (10–50 μg) were separated on 10% or 12% Tris-glycine gels and transferred to polyvinylidene difluoride membranes. Membranes were blocked with 5% non-fat milk in Tris-buffered saline/0.05% Tween-20 for 1.5 h at room temperature and then incubated with primary antibodies against VAMP3 (diluted 1:200; Santa Cruz Biotechnology, CA, USA), VAMP8 (diluted 1:200; Santa Cruz Biotechnology), SNAP23 (diluted 1:500; Abcam, Cambridge, UK), or β-actin (diluted 1:10,000; Bioss, Beijing, China) overnight at 4 °C. After subsequent incubation with secondary antibody, blots were detected by ECL reagent and exposed to X-ray film (Fujifilm, Tokyo, Japan). The signal intensities were quantified using Quantity One software (Bio-Rad, Hercules, California, USA). Target protein expression was normalized to β-actin.

2.10. ELISA

Frozen intestinal and hypothalamic tissues were homogenized in 0.01 M PBS (pH 7.0–7.4) containing 0.1% protease inhibitor. The tissue homogenate and serum were centrifuged at 3000 × *rpm* for 20 min, and the supernatant was collected for cytokine detection. The levels of TNFα, IL6 and IL1β in the intestine, hypothalamus and serum were quantified by ELISA in accordance with the manufacturer's instructions (MEIMIAN, China).

2.11. High-performance liquid chromatography-ultraviolet (HPLC-UV) detection of amino acids

The HPLC-UV method has been described in our previous study [27]. Briefly, frozen intestinal samples (n = 7 each, random samples) were homogenized and suspended in a solution with internal standard (IS; norleucine). After deproteinization and resting, the supernatants were filtered and dehydrated in vacuo, followed by dabsylation with dabsyl chloride reagent. After subsequent dilution and centrifugation,

the supernatants were individually transferred to an insert and injected into an Agilent 1260 HPLC system with a UV detector at 436 nm (Agilent Technologies, USA) coupled with a reverse-phrase C18 column (Hypersil GOLD Thermo, 250 mm × 4 mm ID, 5 μm particle size). The injection volume was 20 μL. Mobile phase A (pH = 6.55) was composed of 9 mM KH2PO4, 4% DMF, 0.1% TEA and 0.055% phosphoric acid. Mobile phase B was a mixture of 80/20 acetonitrile/ultrapure water. Chromatographic separation was performed in a gradient manner. The gradient conditions were as follows: 0–3 min, hold at 8% B; 3–10.5 min, increase to 20% B; 10.5–52.5 min, increase to 35% B; 52.5–67.5 min, increase to 50% B; 67.5–99 min, increase to 100% B; 99–100 min, hold at 100% B; 100–110 min, decrease to 8% B; 110–120 min, hold at 8% B. The run time was 120 min and the flow rate was 1.0 mL/min.

2.12. Statistical analysis

All data were analyzed using SPSS 21.0 (SPSS, Armonk, New York, USA) and plotted with GraphPad Prism 7.0 (La Jolla, CA). For behavioral tests, RT-qPCR, western blotting, ELISA and amino acid detection, Student's *t*-test was used to assess significance. Fisher's exact test was used in functional analysis and pathway analysis. The correlative relationship among cytokines in different tissues was examined using Spearman's rank analysis. Data were expressed as mean ± standard error (SEM), and $P < 0.05$ was considered significant.

3. Results

3.1. CUMS rats display depressive- and anxiety-like behaviors

For the CUMS model, we used body weight and sucrose preference test for baseline evaluation, and no significance was observed prior to the CUMS procedure (Fig. 2B, C). From the second week of CUMS procedure, there was a significant decrease in body weight ($t = -2.322$, $p = 0.026$) and this decrease maintained to the end of the procedure ($t = -3.950$, $p < 0.001$, at the third week; $t = -5.688$, $p < 0.001$, at the forth week; Fig. 2B). And sucrose preference was also significantly decreased ($t = -2.689$, $p = 0.011$, Fig. 2C). In the OFT, no significance was observed in the locomotor activity, calculated by the total distance travelled (Fig. 2D), but the distance travelled in the central zone was significantly decreased in the CUMS group ($t = -2.277$, $p = 0.028$, Fig. 2E). The central activity, indicated by central/total distance, was decreased significantly ($t = -3.008$, $p = 0.005$, Fig. 2F). Immobility time in the FST was markedly increased ($t = 2.976$, $p = 0.005$, Fig. 2G).

3.2. CUMS alters the intestinal protein profile in rats

CUMS rat intestinal samples labeled with iTRAQ-8plex reagents were analyzed by LC-MS/MS. A total of 5652 non-redundant proteins were identified. Using a 1.2-fold change in absolute value as the threshold and $p < 0.05$, 349 unique proteins were found to be significantly changed, with 209 downregulated and 140 upregulated (Supplementary Table S2). A heatmap of the differential proteins, generated using Cluster 3.0 and Treeview, is presented in Fig. 3A, providing a general overview of proteins identified in both groups.

3.3. GO functional annotations and KEGG pathway analyses

GO functional annotations and KEGG pathway analysis were used to further examine the differential proteins. Three categories were covered by GO functional annotations, including “biological process”, “molecular function” and “cellular components”. The top three biological processes were “protein complex assembly”, “angiogenesis involved in wounding healing” and “intracellular protein transport” (Fig. 3B). The top three molecular functions were “poly(A) RNA binding”, “zinc ion binding” and “peptide binding” (Fig. 3C). The top three cellular components were “cytoplasm” ($n = 105$, 22%), “extracellular exosome” ($n = 63$, 13%) and “nuclear” ($n = 58$, 12%) (Fig. 3D).

Based on the KEGG database, the 349 significantly differential proteins were enriched in the following six pathways: “protein digestion and absorption”, “fat digestion and absorption”, “bile secretion”, “carbohydrate digestion and absorption”, “GABAergic synapse” and “basal cell carcinoma” (Fig. 3E).

3.4. Transcript and protein validations of the upregulation of SNAP23, VAMP3 and VAMP8 in the CUMS rat intestine

As mentioned above, “protein complex assembly” was the most significantly affected biological process, and thus, we sought to validate all the differential proteins involved in this process at the transcript level, including *Pf4, Pex14, Snap23, Vamp3, Vamp8 and Slc2a1*. *Snap23* ($t = -2.757$, $p = 0.017$), *Vamp3* ($t = -2.319$, $p = 0.039$) and *Vamp8* ($t = -2.355$, $p = 0.036$) were significantly increased at the transcript level (Fig. 4A). Subsequently, we validated the expression of these three proteins by western blotting. Interestingly, VAMP3 ($t = -2.997$, $p = 0.048$) and VAMP8 ($t = -2.847$, $p = 0.029$) showed significant increases in protein levels, while no difference was observed for SNAP23 (Fig. 4B, C).

3.5. ELISA for cytokine changes in the intestine, serum and hypothalamus

Next, we evaluated the effects of chronic stress on cytokine levels in the intestine, serum and hypothalamus. As shown in Fig. 5A–C, TNFα, IL6 and IL1β levels were all significantly increased in the intestine ($t = -3.920$, $p = 0.003$; $t = -4.253$, $p < 0.001$; $t = -2.479$, $p = 0.023$). In comparison, TNFα levels were decreased in the hypothalamus ($t = 2.259$, $p = 0.042$) and serum ($t = 1.929$, $p = 0.028$). IL1β levels were downregulated in the serum ($t = 2.117$, $p = 0.048$). However, no significant difference was observed in IL6 levels in the hypothalamus or serum, or in IL1β levels in the hypothalamus.

To further investigate whether these cytokine changes in the different tissues are correlated with each other, we performed Spearman rank correlation analysis (Fig. 5D). We observed that TNFα levels in the intestine were negatively correlated with TNFα levels in the hypothalamus and all cytokines measured in the serum. Consistently, IL6 levels in the intestine were negatively correlated with TNFα, IL6 and IL1β in the serum. Moreover, IL1β levels in the intestine were negatively correlated with TNFα and IL1β in the serum. In comparison, TNFα in the hypothalamus was positively correlated with TNFα and IL1β in the serum. Notably, these three cytokines were positively correlated with each other in each tissue.

3.6. Amino acid detection by HPLC shows dysregulation of glutamine, glycine and aspartic acid in the CUMS rat intestine

According to KEGG pathway enrichment analysis, “protein digestion and absorption” was top-ranked, and is involved in amino acid production. Therefore, we examined amino acid content to evaluate the intestinal capacity to digest and absorb proteins. We found that glutamine and glycine were decreased, while aspartic acid was increased (Supplementary table S3). Of note, three upregulated proteins (SLC9A3, ANPEP and LAT1) identified in the proteomics analysis are involved in “protein digestion and absorption”, while three proteins (ASCT2, B^0AT1 and LAT1) validated in our previous study participated in this pathway. Intriguingly, LAT1 was detected by both proteomics and western blotting, with similar changes in levels.

4. Discussion

Recently, much attention has been given to the role of the gut-brain axis in the pathogenesis of depression [10,16,27–29]. Preclinical studies suggest that chronic stress-induced alterations in gut microbiota

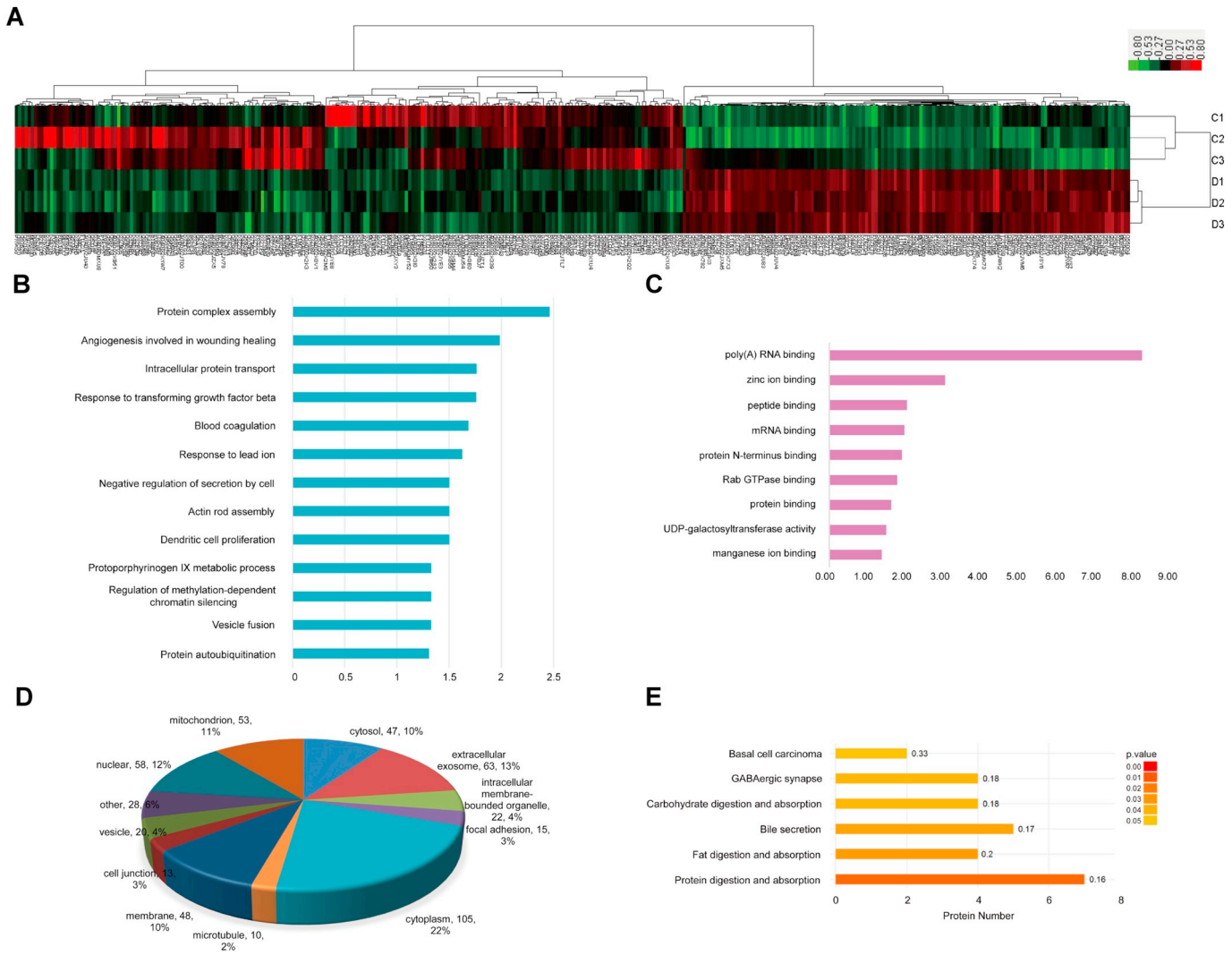

Fig. 3. CUMS alters intestinal protein profile in rats. (A) The heatmap generated by Cluster 3.0 and Treeview presents an overview of the differential intestinal proteins between the CUMS and Control groups. Red indicates upregulated proteins; while green indicates downregulated proteins. (B-D) Functional annotations generated by GO analysis: biological process (B), molecular function (C) and cellular components (D). (E) Significant pathways generated based on the KEGG database. (For interpretation of the references to color in this figure legend, the reader is referred to the web version of this article.)

and host metabolism may contribute to the development of depression [15,27,30]. In the current study, to further explore the role of the intestine in gut-brain bidirectional regulation in depression, we used a shotgun technique, iTRAQ to identify differentially expressed proteins in the intestine of the CUMS rat model. Based on GO functional annotations and validation at the transcript and protein levels, SNAP23, VAMP3 and VAMP8, which are involved in the "protein complex assembly" process, were found to be significantly altered. The cytokines TNFα, IL6 and IL1β were changed in the CUMS rat intestine, serum and hypothalamus. Furthermore, KEGG pathway enrichment analysis and HPLC-UV revealed that amino acid absorption was dysregulated in the CUMS rat intestine.

4.1. Adaptive immune regulation via antigen processing-cross presentation in the ER-phagosome pathway

SNAP23, VAMP3 and VAMP8, were verified by RT-qPCR and western blotting, and all of them showed significant increases at the transcript level in the CUMS rat intestine, although only VAMP3 and VAMP8 were also increased at the protein level. The inconsistencies in SNAP23 transcript and protein levels may be attributed to post-translational modifications, such as phosphorylation [31,32]. It has been reported that SNAP23 interacts with VAMPs and syntaxins to effectuate exocytosis [33,34]. The overall upregulation of these three SNARE components suggests that chronic unpredictable mild stress enhances intestinal mucosal secretion, which is critical in host defense against a variety of pathogens by preventing direct contact with the epithelium [35,36]. A previous study showed that in dendritic cells (DCs), SNAP23 (on the membrane of phagolysosomes) interacts with VAMP3 and VAMP8 (on the membrane of recycling endosomes) to form the SNARE complex, which can promote endoplasmic reticulum compartment (ERC)-phagosome fusion to allow antigen processing-cross presentation [37]. DCs are antigen presenting cells located at mucosal surfaces (such as intestinal mucosa) and lymphoid tissues (such as mesenteric lymph node) to present antigens to T cells via Class I major histocompatibility complex (MHC) [37–39]. The ensuing activation of T cells bolsters the adaptive immune response [39]. Therefore, the simultaneous upregulation of intestinal SNAP23, VAMP3 and VAMP8 found in this study suggests that CUMS enhances the adaptive immune response by promoting antigen processing-cross presentation via the ER-phagosome pathway (Fig. 6A). This immune response might expand from the intestine to elicit a systemic inflammatory response. To test this hypothesis, we measured cytokine levels in the intestine, serum and hypothalamus and found that TNFα, IL6 and IL1β were markedly

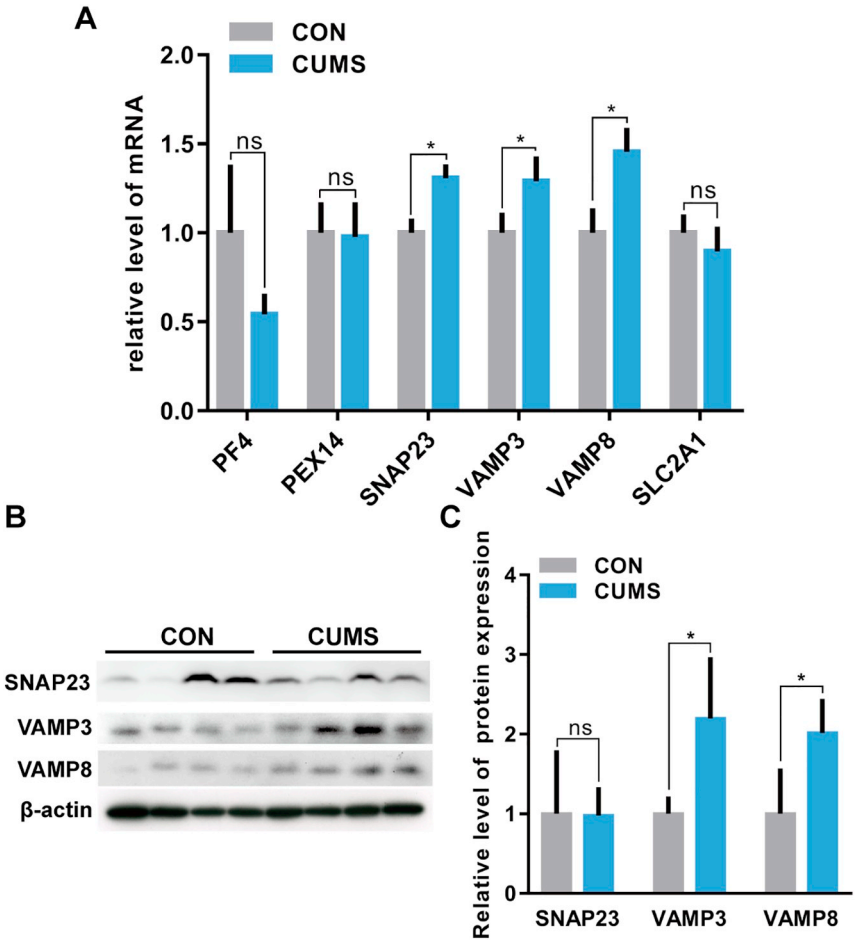

Fig. 4. Effects of CUMS on SNAP23, VAMP3 and VAMP8 expression. (A) In the CUMS intestine, RT-qPCR demonstrated an increase in *Snap23*, *Vamp3* and *Vamp8* mRNA levels ($n = 7$ in the control group; $n = 7$ in the CUMS group). (B–C) Western blots for SNAP23, VAMP3 and VAMP8 revealed a significant increase in VAMP3 and VAMP8 proteins only ($n = 4$ in each group). All data are presented as mean ± SEM. Student's *t*-test; $^*p < 0.05$, ns = no significance. CON, rats in the control group; CUMS, rats in the CUMS group.

dysregulated. These results are consistent with the immune-inflammatory dysregulation previously observed in CUMS mice liver and plasma [22,40], as well as a study in which an anti-inflammatory agent attenuated depressive-like behaviors and the proinflammatory response in CUMS rats [41]. Furthermore, Spearman's correlation analysis revealed a negative correlation between the cytokine changes in the three different tissues, providing further support for the presence of a systemic immune response. Upregulation of cytokines in the intestine may account for the direct contact with gut microbiota, while downregulation of cytokines in the serum and hypothalamus may account for the immunoregulatory inhibition due to long-term low inflammatory stimulus. Thus, the systemic inflammatory response and immune regulation play a critical role in the pathogenesis of depression.

4.2. Disturbance in glutamine, glycine and aspartic acid

Glutamine and glycine were downregulated, while aspartic acid was upregulated in the CUMS rat intestine. The alterations of the intestinal amino acids have been reported in our previous study [27]. Moreover, five differential proteins were found to play an important role in amino acids production and transport (i.e., “protein digestion and absorption” KEGG pathway) (Fig. 6B).

SLC9A3 (NHE3), a Na^+/H^+ exchanger helps form a pH gradient across the apical membrane of the intestinal epithelium, which activates the peptide transporter to deliver di-/tripeptides to the cytoplasm and to complete the ensuing hydrolyzation from peptides to oligopeptides by intracellular peptidases [42,43]. ANPEP (CD13), aminopeptidase N, hydrolyses oligopeptides to single amino acids at the brush-border membrane [44,45]. B^0AT1 (SLC6A19) is a broad specificity neutral amino acid transporter restricted to the apical membrane of the intestine and kidney, and is responsible for absorption of glutamine and glycine [46,47]. ACST2 (SLC1A5) also mediates the influx of glutamine and glycine [48,49]. LAT1 (SLC7A5) acts in a Na+-independent manner and utilizes the intracellular pool of amino acids generated by ASCT2 to exchange a small neutral amino acid (e.g., glutamine) inside for a large essential amino acid (e.g., leucine, tryptophan) outside [50,51]. Their interdependence may account for the coordinated upregulation of these transporters in various disorders, especially cancer [52,53]. LAT1 was not only detected by iTRAQ but also validated by western blotting. Moreover, the consistent trend of this protein by two methods makes the data more reliable. Therefore, it is reasonable to conjecture that the changes in these proteins result in a disturbance in amino acid homeostasis in the CUMS rat intestine. Of note, the intestine samples used for detection by iTRAQ or validation by western blotting are from the same rat cohort. Thus, the results obtained from two methods may supple each other in some kind of degree.

Glutamine is essential for the optimal induction of heat shock proteins to maintain intestinal homeostasis [54]. Glutamine also modulates intestinal cell proliferation and stem cell differentiation [55]. Further, glutamine participates in the central “glutamate/GABA-glutamine cycle” [56,57]. Consistent with the downregulation of glutamine observed in the intestine, decreased levels of glutamine have also been

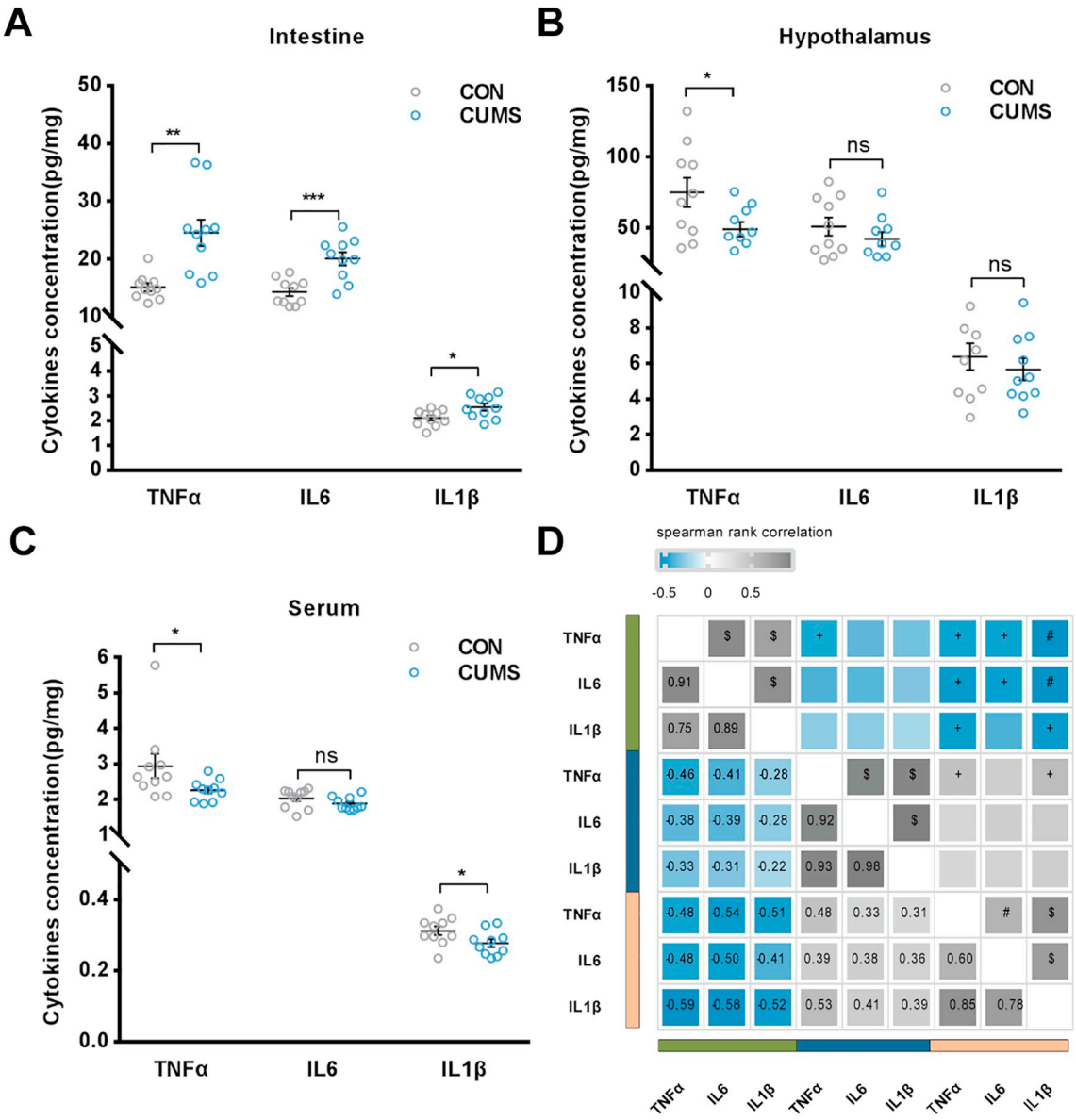

Fig. 5. Effects of CUMS on the levels of cytokines in the intestine, serum and hypothalamus. (A) In the CUMS intestine, the levels of TNFα, IL6 and IL1β were all increased. (B) In the CUMS hypothalamus, the levels of TNFα were decreased while no significant difference was observed in the levels of IL6 and IL1β. (C) In the CUMS serum, the levels of TNFα and IL1β were decreased while no significant difference was observed in the levels of IL6. All data are presented as mean ± SEM. Student's *t*-test; $^{*}p < 0.05$, $^{**}p < 0.01$, $^{***}p < 0.001$, ns = no significance. CON, rats in the control group; CUMS, rats in the CUMS group ($n = 10$ in the control group; $n = 10$ in the CUMS group). (D) Spearman's correlations between TNFα, IL6 and IL1β in the intestine, hypothalamus and serum. Blue indicates a negative correlation; grey indicates a positive correlation. Axis label: green, intestinal cytokines; dark blue, hypothalamic cytokines; light orange, serum cytokines. Numbers on the lower left panel: values of the correlation coefficient; symbols on the upper right panel: results of the significance test; $^{+}p < 0.05$, $^{\#}p < 0.01$, $^{\$}p < 0.001$. (For interpretation of the references to color in this figure legend, the reader is referred to the web version of this article.)

detected in the prefrontal cortex, amygdala and plasma in rodent depressive models [58–60]. Glycine, an agonist of the NMDA receptor in the CNS, is crucial for cognitive function and neuroplasticity in depression [61]. Glycine is increased in the hippocampus of CUMS rats because of a dysfunction in the glycine cleavage system [23]. In contrast to the hippocampus, chronic stress decreases glycine in the periphery (PBMCs and urine) [30,62], similar to the intestine. Aspartic acid regulates dendritic and synaptic proliferation in the CNS [63]. Furthermore, in the enteric nervous system (ENS), L-aspartate is found in L-Asp-immunoreactive neuronal cell bodies and nerve fibers in the myenteric and submucosal plexus of the intestine. Thus, aspartate can modulate neuronal functions in the ENS [64]. We speculate that elevated aspartic acid in the intestine could contribute to ENS dysfunction under chronic stress.

Together, our findings indicate that differential proteins may account for the disturbance in glutamine, glycine and aspartic acid in the intestine of CUMS rats and that perturbations in these amino acids might underlie the pathogenesis of depression.

4.3. Gut-brain axis

Our findings show that CUMS induced adaptive immune response enhancement through ER-phagosome pathway and disturbed amino acids absorption in the intestine. A previous study suggested that chronic stress causes alterations in gut microbiota [15], and TLRs on the intestinal epithelium recognize pathogenic bacteria to trigger an immune response [65,66]. Additionally, psychological stress can directly activate the HPA axis and induce peripheral inflammation [67].

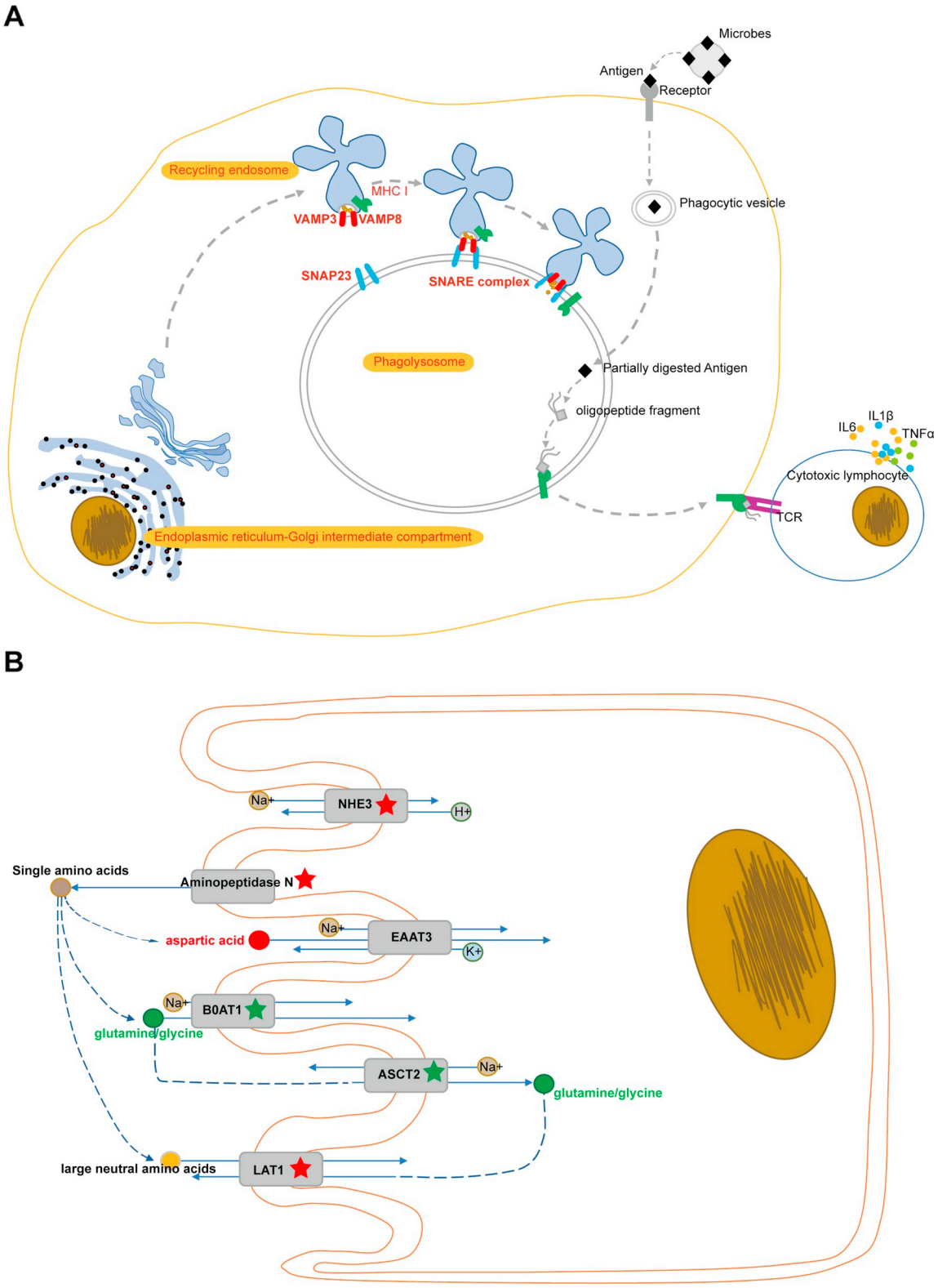

Fig. 6. CUMS induces immunoregulation and disturbed amino acid metabolism in the intestine of rats. (A) SNAP23, VAMP3 and VAMP8 form the SNARE complex, and are involved in the ER-phagosome pathway of antigen processing-cross presentation in the adaptive immune system. (B) CUMS perturbs intestinal glutamine, glycine and aspartic acid absorption in the "protein digestion and absorption" KEGG pathway; the red dot indicates the upregulation of aspartic acid, and the green dots indicate downregulation of glutamine/glycine; the red stars indicate an increase in proteins, while green stars indicate a decrease in proteins; the solid lines show molecular interaction or relation, while the dotted lines show indirect or unknown links. (For interpretation of the references to color in this figure legend, the reader is referred to the web version of this article.)

The gut is an important metabolic site, in which various enzymes function to maintain metabolism balance [68].Notably, certain foods, such as indigestible carbohydrate fibers, require microbial fermentation. Small molecules generated from fermentation are easy to absorb and important for gut-brain bidirectional communication, such as amino acid neurotransmitters and short chain fatty acids [69].

4.4. Limitations

There are several limitations to this study. First, there are several cell types in the intestine, and the proteomic analysis assessed the proteins in all layers of intestine and cell types of the organ. Therefore, further study is needed to identify the locations of the various SNARE complex proteins. Second, the iTRAQ analysis was based on pooled samples, and therefore, individual differences might have been ignored. Thus, a more advanced technique based on individual samples should be used in a future study to obtain more rigorous and thorough information for profiling. Third, our preliminary findings indicated that intestinal SNARE complex proteins involved in the ER-phagosome pathway were altered and cytokines were changed at the systemic level. However, the relationship between the SNARE complex and cytokines is unclear and future study is needed to elucidate the link between them. Last, only proteomic technique was applied in this study and the significance of intestinal physiological and pathological processes in CUMS rats cannot be fully explained, so further study should integrate other omics data, such as metabonomics and transcriptomics.

5. Conclusion

Our findings indicate that CUMS enhances the intestinal adaptive immune response through the ER-phagosome pathway by upregulating the SNARE complex (SNAP23, VAMP3 and VAMP8), and also leads to disturbance in amino acid absorption. These results highlight the key role of gut-brain axis in the pathogenesis of depression and they provide new potential therapeutic targets for this debilitating disorder.

Author contributions

Study concept and design: X.G. and P.X. Performed the experiments: X.G., C.H. and X.Y. Experimental technical guidance: Q.M., L.Z., C.Z., H.W. and B.X. Data analysis: J.C. and P.Z. Manuscripts drafting: X.G. and J.P. All authors reviewed and approved the manuscript prior to its submission.

Declaration of competing interest

The authors declare that they have no conflict of interest.

Acknowledgments

We thank Jane A. Foster, PhD, from McMaster University, St. Joseph's Healthcare, Hamilton, ON, Canada, for critical comments and insightful discussions.

Funding

This work was supported by the National Key Research and Development Program of China (Grant No.2017YFA0505700) and the National Natural Science Foundation of China (Grant No.81701360).

Appendix A. Supplementary data

Supplementary data to this article can be found online at https://doi.org/10.1016/j.lfs.2019.116778.

References

[1] Z. Steel, C. Marnane, C. Iranpour, T. Chey, J.W. Jackson, V. Patel, D. Silove, The global prevalence of common mental disorders: a systematic review and meta-analysis 1980–2013, Int. J. Epidemiol. 43 (2014) 476–493.
[2] H.A. Whiteford, L. Degenhardt, J. Rehm, A.J. Baxter, A.J. Ferrari, H.E. Erskine, F.J. Charlson, R.E. Norman, A.D. Flaxman, N. Johns, R. Burstein, C.J. Murray, T. Vos, Global burden of disease attributable to mental and substance use disorders: findings from the Global Burden of Disease Study 2010, Lancet 382 (2013) 1575–1586.
[3] A. Cipriani, X. Zhou, C. Del Giovane, S.E. Hetrick, B. Qin, C. Whittington, D. Coghill, Y. Zhang, P. Hazell, S. Leucht, P. Cuijpers, J. Pu, D. Cohen, A.V. Ravindran, Y. Liu, K.D. Michael, L. Yang, L. Liu, P. Xie, Comparative efficacy and tolerability of antidepressants for major depressive disorder in children and adolescents: a network meta-analysis, Lancet 388 (2016) 881–890.
[4] J. Keller, R. Gomez, G. Williams, A. Lembke, L. Lazzeroni, G.M. Murphy Jr., A.F. Schatzberg, HPA axis in major depression: cortisol, clinical symptomatology and genetic variation predict cognition, Mol. Psychiatry 22 (2017) 527–536.
[5] H.G. Ruhe, N.S. Mason, A.H. Schene, Mood is indirectly related to serotonin, norepinephrine and dopamine levels in humans: a meta-analysis of monoamine depletion studies, Mol. Psychiatry 12 (2007) 331–359.
[6] W. Wang, H. Guo, S.X. Zhang, J. Li, K. Cheng, S.J. Bai, D.Y. Yang, H.Y. Wang, Z.H. Liang, L. Liao, L. Sun, P. Xie, Targeted metabolomic pathway analysis and validation revealed glutamatergic disorder in the prefrontal cortex among the chronic social defeat stress mice model of depression, J. Proteome Res. 15 (2016) 3784–3792.
[7] O. Berton, C.A. McClung, R.J. Dileone, V. Krishnan, W. Renthal, S.J. Russo, D. Graham, N.M. Tsankova, C.A. Bolanos, M. Rios, L.M. Monteggia, D.W. Self, E.J. Nestler, Essential role of BDNF in the mesolimbic dopamine pathway in social defeat stress, Science (311) (2006) 864–868.
[8] H. N, H. BC, H. K, B. SR, W. GY, S. R, C. A, G. GR, K. V, S. AL, The role of microbiota and inflammation in self-judgement and empathy: implications for understanding the brain-gut-microbiome axis in depression, Psychopharmacology, undefined (2019) (undefined).
[9] Y. Y, T. J, Y. B, Targeting gut microbiome: a novel and potential therapy for autism, Life Sci., 194 (2018) 111–119.
[10] J. Foster, K. McVey Neufeld, Gut-brain axis: how the microbiome influences anxiety and depression, Trends Neurosci. 36 (2013) 305–312.
[11] P. Zheng, B. Zeng, M. Liu, J. Chen, J. Pan, Y. Han, Y. Liu, K. Cheng, C. Zhou, H. Wang, X. Zhou, S. Gui, S.W. Perry, M.-L. Wong, J. Licinio, H. Wei, P. Xie, The gut microbiome from patients with schizophrenia modulates the glutamate-glutamine-GABA cycle and schizophrenia-relevant behaviors in mice, Sci. Adv. 5 (2019) (eaau8317-eaau8317).
[12] N. A, H. K, A. E, S. M, L. A, W. R, R. K, Correlation between the human fecal microbiota and depression, Neurogastroenterology and Motility, 26 (2014) 1155–1162.
[13] J. H, L. Z, Z. Y, M. H, M. Z, Y. Y, W. W, T. W, T. Z, S. J, L. L, R. B, Altered fecal microbiota composition in patients with major depressive disorder, Brain Behav. Immun., 48 (2015) 186–194.
[14] P. AJ, C. J, B. PA, G. JE, V. EF, B. P, C. SM, Altered colonic function and microbiota profile in a mouse model of chronic depression, Neurogastroenterology and Motility 25 (2013) 733–e575.
[15] M. Yu, H. Jia, C. Zhou, Y. Yang, Y. Zhao, M. Yang, Z. Zou, Variations in gut microbiota and fecal metabolic phenotype associated with depression by 16S rRNA gene sequencing and LC/MS-based metabolomics, J. Pharm. Biomed. Anal. 138 (2017) 231–239.
[16] P. Zheng, B. Zeng, C. Zhou, M. Liu, Z. Fang, X. Xu, L. Zeng, J. Chen, S. Fan, X. Du, X. Zhang, D. Yang, Y. Yang, H. Meng, W. Li, N.D. Melgiri, J. Licinio, H. Wei, P. Xie, Gut microbiome remodeling induces depressive-like behaviors through a pathway mediated by the host's metabolism, Mol. Psychiatry 21 (2016) 786–796.
[17] C. HY, N. MX, C. DK, M. WT, Interactions between the gut microbiota and the host innate immune response against pathogens, Front. Immunol., 10 (2019) 607.
[18] L.J. Broom, M.H. Kogut, Gut immunity: its development and reasons and opportunities for modulation in monogastric production animals, Anim. Health Res. Rev. 19 (2018) 46–52.
[19] M.A. Odenwald, J.R. Turner, The intestinal epithelial barrier: a therapeutic target? Nature Reviews Gastroenterology & Hepatology 14 (2016) 9.
[20] M. Lyte, L. Vulchanova, D.R. Brown, Stress at the intestinal surface: catecholamines and mucosa–bacteria interactions, Cell Tissue Res. 343 (2011) 23–32.
[21] C.A. Calarge, S. Devaraj, R.J. Shulman, Gut permeability and depressive symptom severity in unmedicated adolescents, J. Affect. Disord. 246 (2019) 586–594.
[22] Y. Wu, J. Tang, C. Zhou, L. Zhao, J. Chen, L. Zeng, C. Rao, H. Shi, L. Liao, Z. Liang, Y. Yang, J. Zhou, P. Xie, Quantitative proteomics analysis of the liver reveals immune regulation and lipid metabolism dysregulation in a mouse model of depression, Behav. Brain Res. 311 (2016) 330–339.
[23] Z. Y, Y. S, P. J, Y. L, Z. X, L. L, J. X, Z. H, T. T, T. L, X. P, Integrated metabolomics and proteomics analysis of hippocampus in a rat model of depression, Neuroscience, 371 (2018) 207–220.
[24] H. Y, L. W, T. Y, C. X, C. K, X. K, L. C, W. H, Q. C, W. C, L. P, C. H, X. P, iTRAQ-based proteomics suggests LRP6, NPY and NPY2R perturbation in the hippocampus involved in CSDS may induce resilience and susceptibility, Life Sci., 211 (2018) 102–117.
[25] Q. Mao, X. Gong, C. Zhou, Z. Tu, L. Zhao, L. Wang, X. Wang, L. Sun, J. Xia, B. Lian, J. Chen, J. Mu, D. Yang, P. Xie, Up-regulation of SIRT6 in the hippocampus induced rats with depression-like behavior via the block Akt/GSK3beta signaling pathway,

Behav. Brain Res. 323 (2017) 38–46.
[26] L. Liu, X. Zhou, Y. Zhang, J. Pu, L. Yang, S. Yuan, L. Zhao, C. Zhou, H. Zhang, P. Xie, Hippocampal metabolic differences implicate distinctions between physical and psychological stress in four rat models of depression, Transl. Psychiatry 8 (2018) 4.
[27] Y. X, W. G, G. X, H. C, M. Q, Z. L, Z. P, Q. Y, Y. F, L. B, Z. C, W. H, Z. W, X. P, Effects of chronic stress on intestinal amino acid pathways, Physiol. Behav., 204 (2019) 199–209.
[28] K. M, W.-S. U, A. M, L. W, M. U, Abdominal vagal deafferentation alters affective behaviors in rats, J. Affect. Disord., 252 (2019) 404–412.
[29] E. A, C. ME, The gut-brain axis: the missing link in depression, Clinical Psychopharmacology and Neuroscience, 13 (2015) 239–244.
[30] M. W, S. J, W. H, S. F, Z. N, J. J, X. Y, Z. L, Y. L, Z. M, Chronic paradoxical sleep deprivation-induced depression-like behavior, energy metabolism and microbial changes in rats, Life Sci., 225 (2019) 88–97.
[31] G. Hu, A.Y. Gong, A.L. Roth, B.Q. Huang, H.D. Ward, G. Zhu, N.F. Larusso, N.D. Hanson, X.M. Chen, Release of luminal exosomes contributes to TLR4-mediated epithelial antimicrobial defense, PLoS Pathog. 9 (2013) e1003261.
[32] Y. Wei, D. Wang, F. Jin, Z. Bian, L. Li, H. Liang, M. Li, L. Shi, C. Pan, D. Zhu, X. Chen, G. Hu, Y. Liu, C.Y. Zhang, K. Zen, Pyruvate kinase type M2 promotes tumour cell exosome release via phosphorylating synaptosome-associated protein 23, Nat. Commun. 8 (2017) 14041.
[33] V. Ravichandran, A. Chawla, P.A. Roche, Identification of a novel syntaxin- and synaptobrevin/VAMP-binding protein, SNAP-23, expressed in non-neuronal tissues, J. Biol. Chem. 271 (1996) 13300–13303.
[34] C.C. Wang, H. Shi, K. Guo, C.P. Ng, J. Li, B.Q. Gan, H. Chien Liew, J. Leinonen, H. Rajaniemi, Z.H. Zhou, Q. Zeng, W. Hong, VAMP8/endobrevin as a general vesicular SNARE for regulated exocytosis of the exocrine system, Mol. Biol. Cell 18 (2007) 1056–1063.
[35] T. Pocard, A. Le Bivic, T. Galli, C. Zurzolo, Distinct v-SNAREs regulate direct and indirect apical delivery in polarized epithelial cells, J. Cell Sci. 120 (2007) 3309–3320.
[36] S. Cornick, F. Moreau, H.Y. Gaisano, K. Chadee, Entamoeba histolytica-induced mucin exocytosis is mediated by VAMP8 and is critical in mucosal innate host defense, mBio 8 (2017).
[37] N.-G. P, B. A, T. N, S. F, F. O, H. Y, B. M, O. M, R. PA, T. R, B. BD, A. D, W. SW, B. JM, TLR signals induce phagosomal MHC-I delivery from the endosomal recycling compartment to allow cross-presentation, Cell 158 (2014) 506–521.
[38] S. I, G. AG, S. R, M. E, D.-R. P, T. C, Identification of CD8α dendritic cells in rainbow trout (Oncorhynchus mykiss) intestine, Fish & shellfish immunology 89 (2019) 309–318.
[39] G. SJ, K. P, Cross-talk between antigen presenting cells and T cells impacts intestinal homeostasis, bacterial infections, and tumorigenesis, Front. Immunol., 10 (2019) 360.
[40] C. Yang, C. Zhou, J. Li, Z. Chen, H. Shi, W. Yang, Y. Qin, L. Lü, L. Zhao, L. Fang, H. Wang, Z. Hu, P. Xie, Quantitative proteomic study of the plasma reveals acute phase response and LXR/RXR and FXR/RXR activation in the chronic unpredictable mild stress mouse model of depression, Mol. Med. Rep. 17 (2018) 93–102.
[41] S. Y, S. R, J. Z, L. X, F. Q, M. S, Perilla aldehyde attenuates CUMS-induced depressive-like behaviors via regulating TXNIP/TRX/NLRP3 pathway in rats, Life Sci. 206 (2018) 117–124.
[42] K. DJ, L. FH, G. V, T. DT, Optimal absorptive transport of the dipeptide glycylsarcosine is dependent on functional Na+/H+ exchange activity, Pflugers Archiv 445 (2002) 139–146.
[43] A. CM, T. DT, Regulation of intestinal hPepT1 (SLC15A1) activity by phosphodiesterase inhibitors is via inhibition of NHE3 (SLC9A3), Biochim. Biophys. Acta 1768 (2007) 1822–1829.
[44] M. R, Cell-surface peptidases, Int. Rev. Cytol. 235 (2004) 165–213.
[45] M.-O. P, The moonlighting enzyme CD13: old and new functions to target, Trends Mol. Med. 14 (2008) 361–371.
[46] B. S, Amino acid transport across mammalian intestinal and renal epithelia, Physiol. Rev. 88 (2008) 249–286.
[47] B. S, Apical transporters for neutral amino acids: physiology and pathophysiology, Physiology (Bethesda, Md.), 23 (2008) 95–103.
[48] D. R, S. Y, F. C, B. A, B. A, L. MP, Luminal leptin inhibits L-glutamine transport in rat small intestine: involvement of ASCT2 and B0AT1, Am. J. Physiol. Gastrointest. Liver Physiol. 299 (2010) G179–G185.
[49] U.-T. N, E. H, K. Y, Cloning and functional characterization of a system ASC-like Na+-dependent neutral amino acid transporter, J. Biol. Chem. 271 (1996) 14883–14890.
[50] P.J. Bothwell, C.D. Kron, E.F. Wittke, B.N. Czerniak, B.P. Bode, Targeted suppression and knockout of ASCT2 or LAT1 in epithelial and mesenchymal human liver cancer cells fail to inhibit growth, Int. J. Mol. Sci. 19 (2018) 2093.
[51] A. J, Z. M, Exchange-mode glutamine transport across CNS cell membranes, Neuropharmacology, undefined (2019) (undefined).
[52] W. Q, B. KA, O. NJ, F. J, B. CG, v.G. M, S. DM, T. JC, R. RM, J. M, H. NK, R. JE, H. J, Targeting glutamine transport to suppress melanoma cell growth, Int. J. Cancer, 135 (2014) 1060–1071.
[53] E.-A. R, C. ML, A. L, S. D, D.-R. M, N. CC, E. IO, R. EA, G. AR, The combined expression of solute carriers is associated with a poor prognosis in highly proliferative ER+ breast cancer, Breast Cancer Res. Treat. 175 (2019) 27–38.
[54] I. Y, S. T, M. MW, R. MJ, T. H, C. EB, Polyamines mediate glutamine-dependent induction of the intestinal epithelial heat shock response, Am. J. Physiol. Gastrointest. Liver Physiol. 301 (2011) G181–G187.
[55] C.S., X.Y., Z.G., Y.J., T.C., D.B., D.J., Y.Y., R.W., Glutamine supplementation improves intestinal cell proliferation and stem cell differentiation in weanling mice, Food Nutr. Res., 62 (2018) (undefined).
[56] d.L. DS, M. LM, B.E. A, D.R. A, d.S. LS, G. RC, L-glutamine supplementation during the lactation period facilitates cortical spreading depression in well-nourished and early-malnourished rats, Life Sci. 85 (2009) 241–247.
[57] C. Zhao, S.C. Gammie, Glutamate, GABA, and glutamine are synchronously upregulated in the mouse lateral septum during the postpartum period, Brain Res. 1591 (2014) 53–62.
[58] M. K, S. Y, H. M, I. M, H. K, Differential levels of brain amino acids in rat models presenting learned helplessness or non-learned helplessness, Psychopharmacology, 229 (2013) 63–71.
[59] P. VV, N. TB, C. Y, O. YE, P. YH, B. HM, K. JY, S. KH, K. JH, L. KH, C. YC, Metabolite signature associated with stress susceptibility in socially defeated mice, Brain Res. 1708 (2019) 171–180.
[60] C. YP, W. C, X. JP, Chronic unpredictable mild stress induced depression-like behaviours and glutamate-glutamine cycling dysfunctions in both blood and brain of mice, Pharm. Biol., 57 (2019) 280–286.
[61] P. B, R. JD, P. Z, I. M, B. E, M. RS, The glycine site of NMDA receptors: a target for cognitive enhancement in psychiatric disorders, Prog. Neuro-Psychopharmacol. Biol. Psychiatry 92 (2019) 387–404.
[62] J. Li, G. Tang, K. Cheng, D. Yang, G. Chen, Z. Liu, R. Zhang, J. Zhou, L. Fang, Z. Fang, X. Du, P. Xie, Peripheral blood mononuclear cell-based metabolomic profiling of a chronic unpredictable mild stress rat model of depression, Mol. BioSyst. 10 (2014) 2994–3001.
[63] P. TB, C. JB, Synthesis of N-acetyl-L-aspartate by rat brain mitochondria and its involvement in mitochondrial/cytosolic carbon transport, The Biochemical Journal 184 (1979) 539–546.
[64] N. M, M. N, S. R, L-aspartate-immunoreactive neurons in the rat enteric nervous system, Cell Tissue Res. 318 (2004) 483–492.
[65] H. JY, L. SS, H. TY, L. ZQ, Y. D, Y. HQ, G. L, W. GH, Z. HT, L. ZG, Y. PC, Frontline science: TLR3 activation inhibits food allergy in mice by inducing IFN-γ Foxp3 regulatory T cells, J. Leukoc. Biol. (2019), https://doi.org/10.1002/JLB.3HI0918-348RR.
[66] A.B. S, K. SH, I. SH, S. SD, Induction effects of Bacteroides fragilis derived outer membrane vesicles on toll like receptor 2, toll like receptor 4 genes expression and cytokines concentration in human intestinal epithelial cells, Cell J., 21 (2019) 57–61.
[67] H. MA, Z. PA, A. C, M. K, P. CM, Glucocorticoids and inflammation: a double-headed sword in depression? How do neuroendocrine and inflammatory pathways interact during stress to contribute to the pathogenesis of depression?, Modern trends in pharmacopsychiatry, 28 (2013) 127–143.
[68] N. ML, P. RS, B. LN, R. SB, H. VS, A. AU, Early metabolic changes in the gut leads to higher expression of intestinal alpha glucosidase and thereby causes enhanced postprandial spikes, Life Sci., 218 (2019) 8–15.
[69] A. Farzi, A.M. Hassan, G. Zenz, P. Holzer, Diabesity and mood disorders: multiple links through the microbiota-gut-brain axis, Mol. Asp. Med. 66 (2019) 80–93.